

Improved Load Shedding Scheme considering Distributed Generation

Das, Kaushik; Nitsas, Antonios; Altin, Müfit; Hansen, Anca Daniela; Sørensen, Poul Ejnar

Published in:
I E E E Transactions on Power Delivery

Link to article, DOI:
[10.1109/TPWRD.2016.2536721](https://doi.org/10.1109/TPWRD.2016.2536721)

Publication date:
2017

Document Version
Peer reviewed version

[Link back to DTU Orbit](#)

Citation (APA):
Das, K., Nitsas, A., Altin, M., Hansen, A. D., & Sørensen, P. E. (2017). Improved Load Shedding Scheme considering Distributed Generation. I E E E Transactions on Power Delivery, 32(1), 515-524. DOI: 10.1109/TPWRD.2016.2536721

DTU Library

Technical Information Center of Denmark

General rights

Copyright and moral rights for the publications made accessible in the public portal are retained by the authors and/or other copyright owners and it is a condition of accessing publications that users recognise and abide by the legal requirements associated with these rights.

- Users may download and print one copy of any publication from the public portal for the purpose of private study or research.
- You may not further distribute the material or use it for any profit-making activity or commercial gain
- You may freely distribute the URL identifying the publication in the public portal

If you believe that this document breaches copyright please contact us providing details, and we will remove access to the work immediately and investigate your claim.

Improved Load Shedding Scheme considering Distributed Generation

Kaushik Das, *Student Member, IEEE*, Antonios Nitsas, Müfit Altin, *Member, IEEE*, Anca D Hansen, *Member, IEEE*, and Poul E Sørensen, *Senior Member, IEEE*

Abstract—With high penetration of distributed generation (DG), the conventional under-frequency load shedding (UFLS) face many challenges and may not perform as expected. This article proposes new UFLS schemes, which are designed to overcome the shortcomings of traditional load shedding scheme. These schemes utilize directional relays, power flow through feeders, wind and PV measurements to optimally select the feeders to be disconnected during load shedding such that DG disconnection is minimized while disconnecting required amount of consumption. These different UFLS schemes are compared in terms of frequency response, amount of consumption and DG disconnected during load shedding.

Index Terms—Under-frequency load shedding, distributed generation, optimization

NOMENCLATURE/SYMBOL

WT	wind turbine
PV	photovoltaic
DG	distributed generation
UFLS	under-frequency load shedding
TSO	transmission system operator
DSO	distribution system operator
RMSE	root mean square error
NRMSE	normalised root mean square error
$freq$	frequency.
$freq_0$	nominal frequency (50 Hz for test system).
RoCoF	rate of change of frequency also denoted as $dfreq/dt$
P	active power in MW.
P_0	active power at nominal frequency $freq_0$ in MW.
Q	reactive power in MVAR.
Q_0	reactive power at nominal frequency $freq_0$ in MVAR.
K_{pf}	frequency sensitivity parameter w.r.t P
K_{qf}	frequency sensitivity parameter w.r.t Q
t	t^{th} time instant
m	measurement
f	forecast
i	i^{th} feeder
Σ	sum for all the feeders
C	consumption in MW
W	wind generation in MW
S	solar PV generation in MW
k	load shedding stage number

A	consumption to be disconnected in each load shedding stage in %
x	vector representing the switching status of the feeders
v	wind speed
I	solar insolation
η	gaussian distribution of error
μ	mean of η
σ	standard deviation of η
\underline{n}	unknown vector for DG Estimation
\underline{g}	measurement vector for DG Estimation
\underline{E}	matrix of co-efficients between measurement and unknown vectors
Sc	score or priority for the feeders
e	estimate

I. INTRODUCTION

THE penetration of renewable generation has been increasing significantly all over the world, and expected to reach more than 20% of the total system generation in Europe by 2020 [1]. High proportion of these generation units are connected to the distribution systems and are referred to as Distributed Generations (DGs). The integration of DGs in the power systems offers several benefits, like reducing congestions and losses in the lines and feeders. Due to improvement in technologies and reducing costs, renewable energy sources are becoming more common choices among the DG options. This also has added benefit of low environmental impact. However, high penetration of DG like wind generations and PV generations may also challenge reliability and security of power system.

In order to have stable operation of a power system, it is essential to keep the frequency within the nominal operating ranges. However, a severe disturbance like loss of a large generating unit can cause fast decline of frequency which can result in frequency instability. In order to limit the frequency from going too low, frequency containment reserves are deployed from dedicated generators. If these reserves are exhausted or unable to contain the frequency, the system enters in an emergency state. Special defence strategies employing system protection schemes called special protection systems (SPS) are employed to defend against instabilities in emergency state. Under-frequency load shedding is one such SPS which is considered as last resort to prevent frequency instability [2]. ENTSO-E recommendation for UFLS for European networks is shown in Fig. 1 [3]. It can be observed from

Kaushik Das, Antonios Nitsas, Müfit Altin, Anca D Hansen and Poul E Sørensen are with Wind Energy Department, Technical University of Denmark, Risø, Roskilde, 4000 Denmark e-mail: kdas@dtu.dk

Fig. 1 that minimum load shedding is recommended to start at 49 Hz and multiple steps of load shedding are continued until 48.1 Hz as represented by the red region. However, load shedding from 49.2 until 48.6 (as represented by the green region) is desirable.

Although it should be noted that UFLS is the last resort to contain frequency decline and it causes economic loss and consumer discomfort. UFLS is generally performed by automatically disconnecting the feeders at distribution substations. Disconnecting feeders with large penetration of DG may disconnect substantial amount of generation. Consequently, the required amount of load disconnection as per design requirements (e.g. Fig. 1) is not achieved. Traditional load shedding relays do not consider this effect. Thus high penetration of DG advocates for advanced UFLS approach which would take DG into account [4].

In literature, there have been several works on UFLS. Delfino

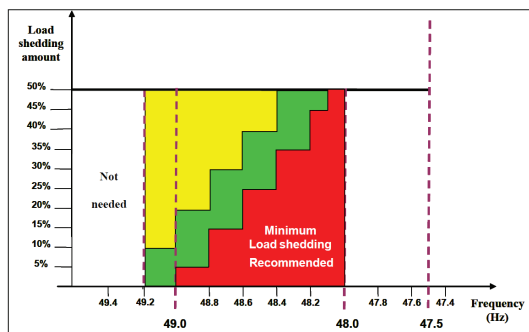


Fig. 1. ENTSO-E Recommendation for UFLS

et. al. [5] have compared traditional, semi-adaptive and adaptive load shedding schemes. Anderson et. al. [6], Rudez et. al. [7], [8] proposed an adaptive UFLS scheme using rate of change of frequency. Terzija [9] proposed an adaptive UFLS scheme considering magnitude of disturbance. Ceja-Gomez et. al. [10] solved UFLS problem using integer programming whereas, Luan et. al. [11] used genetic algorithm. Manson et. al. [12] have provided a case study of UFLS scheme considering communication challenges as well. Reddy et. al. [13] uses PMU based sensitivity study to find location and amount of load to be shed. Mullen et. al. [14] and [15] proposed smart grid approaches for UFLS. However, these UFLS schemes do not take into account effects of high penetration of DG in their schemes. Therefore, during load shedding these methods may disconnect substantial amount of DG.

Recently some works have been done regarding UFLS considering DG. Liu et. al. [16] proposed an UFLS method where DG provides active power support to alleviate under-frequency problem. Xu et. al. [17] classified DG into different categories for their applicability for UFLS. Malekpour et. al. [18] optimized loads and losses to be minimum with integration of DG. Mahat et. al. [19] stabilized the frequency in an islanded system consisting of DG. However, all these methods suffer from an important drawback that none of these methods consider that if substantial amount of DG is disconnected during UFLS, frequency response will be very

poor and may lead to frequency instability in extreme cases. These methods do not consider amount of DG connected to any feeder before disconnecting it. "IEEE Guide for the Application of Protective Relays Used for Abnormal Frequency Load Shedding and Restoration" [4], has clearly mentioned that tripping feeders that have active DG certainly diminishes the beneficial affect of load shedding, and can even have negative impact by eliminating sources of generation that supports system inertia. Therefore, in this article, novel load shedding schemes are developed which try to minimize the amount of DG disconnection while disconnecting the required amount of consumptions.

This article develops and compares different new UFLS schemes which take into consideration the amount of DG connected to the feeders in real-time. These UFLS schemes basically are - i) traditional method using static relay ii) directional relay based UFLS using power flow direction in the feeders, iii) novel UFLS scheme using power flow magnitude and direction, iv) novel UFLS scheme using power flow and DG data respectively. In order to use DG data, amount of DG connected to each feeder are estimated using power flow data. Based on the real-time estimation of the amount of DG connected, each feeder is prioritized for UFLS. Following prioritization, feeders are selected for load shedding. It has been observed that this selection of feeders is a combinatorial optimization problem. These methods are studied and compared on a test transmission system in which distribution networks are incorporated. In order to validate the results over large wind and PV generation scenarios, monte carlo simulations [20] are run.

The paper is organised as following: Section II describes the power system model. Section III discusses different load shedding schemes. Section IV provides the results from the simulations. Section V concludes the paper.

II. POWER SYSTEM MODEL

The transmission network model developed by Akhmatov et. al. [21] (as shown in Fig. 2) is used for studies. Total generation capacity of this synthetic transmission system is 7080 MW whereas demand of the system is 6060 MW. In order to study the effects of load shedding on this transmission system, 4 different loads (LD1, LD2, LD3 and LD4) as shown in Fig. 2 at 4 different locations in the network are replaced with distribution networks. Distribution networks can be represented with aggregated feeders as discussed by Goksu et. al. [22]. In this paper, distribution networks are modelled as combination of feeders with aggregated loads, PV generation and wind generation in each feeders as shown in Fig. 3. This distribution system is modelled as a 110 kV substation where loads are modelled as aggregated loads connected to 11 20 kV feeders. 6 of these feeders are connected to residential loads, 4 feeders are connected to commercial loads and 1 feeder has industrial loads connected to it.

Wind generations are modelled as IEC 61400-27 Type 1 generic wind turbine [23] and PV generations are modelled using standard models provided by DigSilent PowerFactory [24]. However, it should be noted that the model as well as

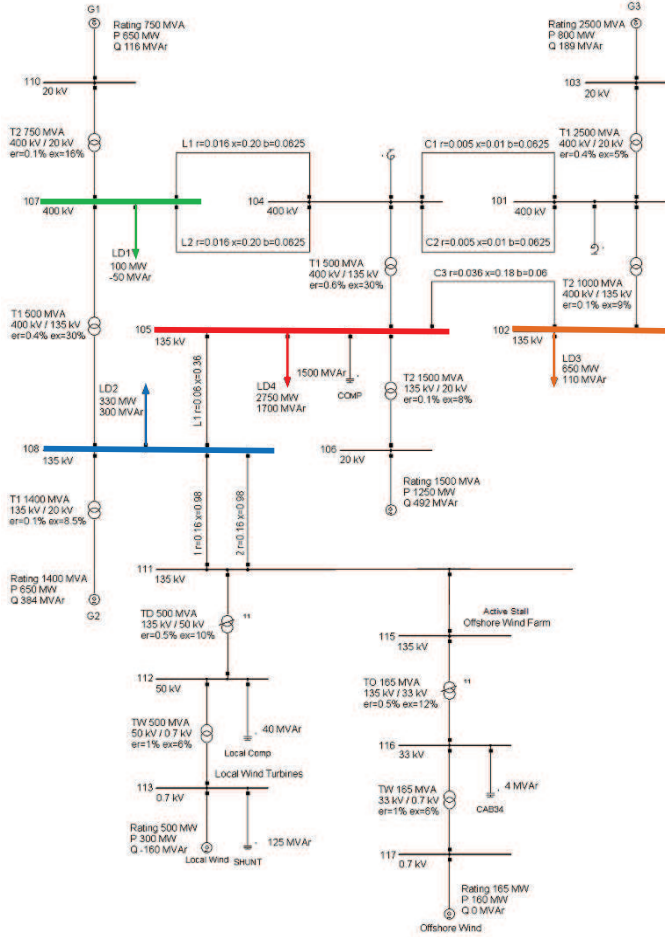


Fig. 2. Transmission System Model [21]

the developed UFLS scheme is generic for any distribution network. Frequency dependencies of active and reactive power of different types of loads are designed as:

$$P = P_0[1 + K_{pf}(freq - freq_0)] \quad (1)$$

$$Q = Q_0[1 + K_{qf}(freq - freq_0)] \quad (2)$$

Frequency parameters, K_{pf} and K_{qf} for different types of loads are given in Table I.

TABLE I
TYPICAL LOAD FREQUENCY PARAMETERS

Load Type	Frequency Parameters	
	K_{pf}	K_{qf}
Residential		
Electrical Heating	1	-1.7
Non Electrical Heating	0.8	-1.7
Commercial		
Electrical Heating	1.5	-1.1
Non Electrical Heating	1.7	-0.9
Industrial	2.6	1.6

Four different distribution system networks are connected at four different locations as shown in Fig. 2. Wind speed and

hence available wind power generation for these 4 different locations are modelled using CorWind model [25]. Whereas, PV generation are modelled based on the data provided by Belgian TSO, ELIA for different locations in Belgium network [26]. Under-frequency disconnection settings of the DG is set on 47.5 Hz according to the ENTSO-E Network Code Requirements for Connection [27]; the grid code connection requirements for small generators in Denmark (current rating 16 A or lower) [28] and the grid code connection requirements for Wind and PV plants above 11 kW in Denmark [29], [30]. Disconnection of a large generator in the transmission network is simulated in order to simulate large frequency drop in the system. The UFLS scheme is designed in this article based on the minimum load shedding recommendations as shown in Fig. 1. The applied settings are given in Table II. Frequency

TABLE II
RECOMMENDATION FOR UNDER-FREQUENCY LOAD SHEDDING

Stage(k)	Frequency [Hz]	Minimum Load Shedding Amount(A_k)
1	49	5%
2	48.8	10%
3	48.6	10%
4	48.4	10%
5	48.2	10%
6	48.1	5%

and Rate of Change of Frequency (RoCoF) measurements are computed using a moving average filter as described in IEC 61400-27-1 standard [23].

III. DIFFERENT LOAD SHEDDING SCHEMES

4 load shedding schemes and their advantages/disadvantages are described in the following:

A. Load Shedding Algorithm using Static Relay (LSA-Static)

Traditionally static relays are installed in selected feeders based on amount of installed loads in these feeders [4], [31]. Traditionally, a certain number of feeders are selected based on the historical measured load data of these feeders such that their disconnection should disconnect the required amount of load. For example, among the regional reliability councils of North American Electric Reliability Council (NERC), SERC Reliability Corporation requires that these load shedding strategies should have the capability of shedding certain percent of demand at the time coincident with the previous year actual peak demand [32], whereas Southwest Power Pool (SPP) requires to shed certain percentage of the forecasted peak load [33]. Generally these feeders are chosen based on types of loads connected to the feeders, network topology, equal distribution of loads to be shed etc. [34]. Although this scheme is very simple and inexpensive to implement, it is sub-optimal. In case there is substantial amount of DG connected to these selected feeders, it may not disconnect required amount of consumption. Consequently, frequency response may deteriorate resulting in activation of larger number of load shedding stages. Therefore, at the end it may disconnect larger amount of load than required. Another major drawback of this scheme is that it may disconnect substantial amount of DG.

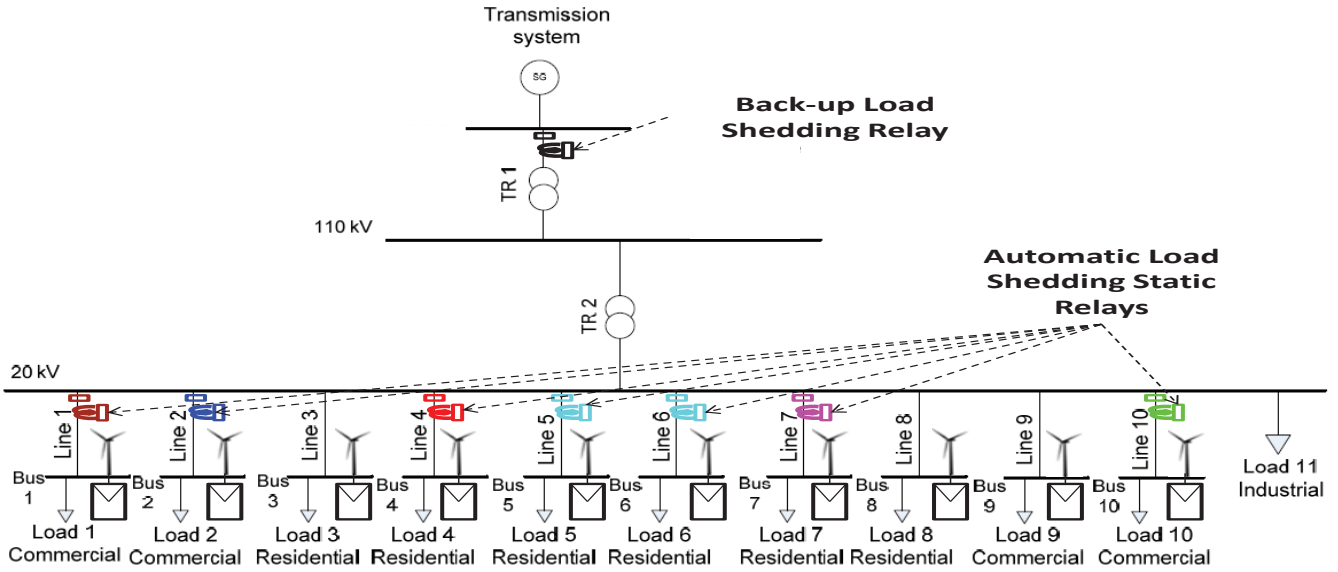


Fig. 3. Distribution System Model

This is not desirable since disconnecting generation during an under-frequency emergency will not reduce the required amount of consumption. Consequently, the frequency may keep falling down making the system vulnerable to under-frequency instability.

As shown in Table II, the feeders in the system are expected to be disconnected to disconnect a predefined amount of demand, e.g. 10% of the demand should be disconnected at a frequency of 48.8 Hz [3]. In this article, this scheme is considered as the baseline scheme to which the performance of other load shedding schemes are compared. The locations of these UFLS relays are given in Table III and shown in Fig. 3. In this scheme, feeder with industrial load of Fig. 3 is not considered for load shedding (i.e. given very high priority). This feeder with industrial load represents all the high priority feeders in a practical distribution networks which are excluded from load shedding. In our studies equal priorities are given to the feeders with commercial and residential loads.

TABLE III
LOAD SHEDDING SETTINGS FOR STATIC RELAYS

Stage(k)	Frequency [Hz]	Amount(A_k)	Locations
1	49	5%	Line 4
2	48.8	10%	Line 2
3	48.6	10%	Line 10
4	48.4	10%	Line 5,6
5	48.2	10%	Line 1
6	48.1	5%	Line 7

B. Load Shedding Algorithm using Static Relay with Directional element (LSA-Directional)

One of the major drawback of the load shedding scheme using static relay is that it may disconnect substantial amount of DG while disconnecting specific feeders. It is possible that at certain time of the day, generations from DG can be higher than consumption for any of these feeders. As a result,

the feeder acts as a generator instead of load. Disconnecting any such feeder can have detrimental effects on the system frequency. In order to prevent such scenarios, a directional power relay element can be incorporated along with the static relays. This relay checks whether the power flow in the feeder is from distribution network to transmission network. If power is flowing from distribution network to transmission network then the relay is blocked from activation and the corresponding feeder is not disconnected.

Although this scheme is expected to perform better than LSA-Static scheme, it is not optimal, as it can disconnect substantial amount of DG and not disconnect required amount of consumption.

C. Load Shedding Algorithm using Power Flow (LSA-PF)

This scheme considers the actual value of power that flows in each feeder along with the direction of the power flow. The inputs of LSA-PF are the measured frequency, the RoCoF and the measured active power flows of all the distribution feeders. It is assumed that the total consumption forecast in the concerned distribution network is available from TSO. The flowchart for the scheme is shown in Fig. 4. Power flow measurements for all the feeders, $P_{m,i,t}$ are used to select the feeders for disconnection. It can be observed from Fig. 4 that if any feeder produces more active power than what it consumes i.e. power flow is negative, it is not considered for disconnection. Frequency measurements, $freq_{m,t}$ are used to find out if frequency is less than load shedding activation frequency, $freq_k$ (Table II) and RoCoF ($(dfreq/dt)_{m,t}$) is negative then “Feeder Selection Algorithm” (discussed below) is run. RoCoF is basically used to identify whether the frequency is going down or going up. Filtering of the RoCoF signal is necessary due to the noise generated by differentiating frequency. Moving Average filter is applied as given in [23].

Feeder Selection Algorithm is described in the following. As depicted in Table II, the required amount of load to shed

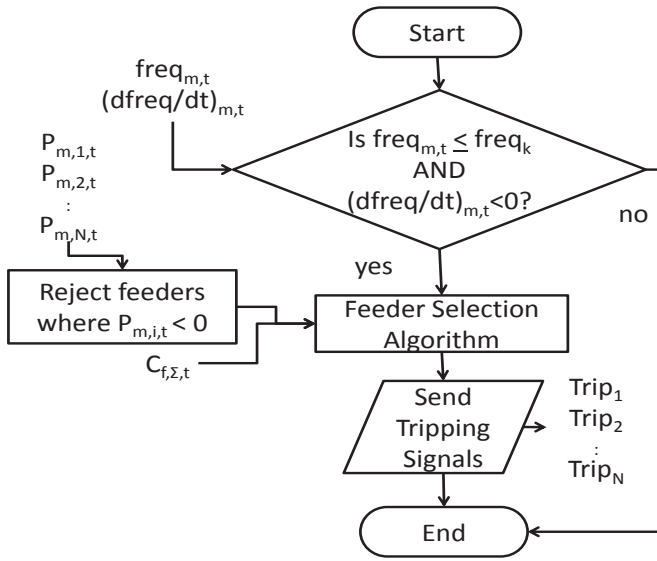


Fig. 4. Flowchart for Load Shedding using Power Flow

is different, being dependent on frequency stage. Therefore, the algorithm finds the feeder or the combination of feeders that have the minimum amount of active power flow greater than 5% or 10% (denoted by A_k) of the total consumption, depending on the load shedding stage.

The amount of consumption needed to be disconnected for load shedding stage k is given by (3):

$$C_{\Sigma,k,t,shed} = C_{f,\Sigma,t} * A_k \quad (3)$$

The total consumption needed to be disconnected, $C_{\Sigma,k,t,shed}$ is calculated based on the consumption forecast for the distribution network obtained from TSO, $C_{f,\Sigma,t}$. It is assumed to have low error since consumption does not generally have large variation in considered time window of 5 minutes.

Feeder Selection Algorithm finds out the feeders for which the sum of the power flows is greater and as close as possible to the total consumption to be disconnected, $C_{\Sigma,k,t,shed}$. This is basically a combinatorial optimization problem which can be modelled as “0/1 Knapsack Problem” [35].

“0/1 Knapsack Problem” for Feeder Selection Algorithm can be modelled as following:

$$\begin{aligned} \max \quad & \sum_{i=1}^{total_num_feeders} -P_{m,i,t} * x_{i,t} \\ \text{subject to} \quad & \sum_{i=1}^{total_num_feeders} -P_{m,i,t} * x_{i,t} \leq -C_{\Sigma,k,t,shed} \\ & x_{i,t} \in \{0,1\} \end{aligned} \quad (4)$$

The objective function is to minimize the sum of the power flows through selected combination of feeders subject to the constraint that the sum of the power flows through selected combination of feeders is greater than the total consumption to be disconnected. x_i represents the switching status of the feeders. x_i is 1 if the feeder should be disconnected or 0 otherwise. The binary vector solution \underline{x} to the (4) indicates

which feeders to be disconnected based on which signals to trip the relays are sent. However, it should be noted that since “0/1 Knapsack Problem” is a integer programming problem, therefore $P_{m,i,t}$ and $C_{\Sigma,k,t,shed}$ are appropriated up to the second decimal point.

This load shedding scheme has the advantages of improved frequency response as compared to load shedding using static relays. This scheme disconnects at least the required amount of consumption but since this method does not use DG data it may disconnect substantial amount of generation resulting in shedding more consumption than required.

D. Load Shedding Algorithm using DG data (LSA-DG)

In order to handle the disadvantage of the previous scheme, a new scheme is developed. This scheme uses the estimate of the amount of distributed PV and wind generation (described later) connected to each feeder. Based on these estimates, all the feeders are prioritized. The feeder selection algorithm selects the feeders to be disconnected considering the priorities (described later). The flowchart for this scheme is shown in the Fig. 5.

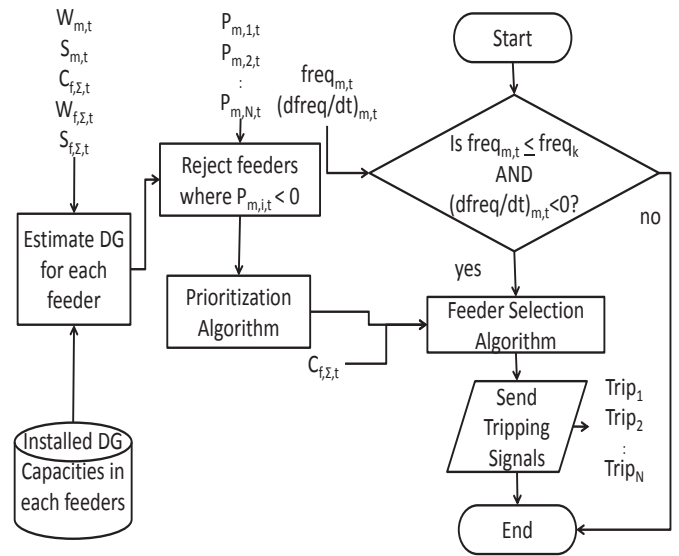


Fig. 5. Flowchart for Load Shedding using DG Data

DG Estimation: It should be noted here that the objective of this paper is not to accurately estimate the amount of DG connected to each feeder. If any other estimation algorithm is available it can be readily used. However, it is also important to keep in mind that any error in estimation algorithm only introduces error in prioritization of feeders for disconnection, resulting in a small error while disconnecting the feeders. Therefore, prioritization algorithm is kept robust enough to take account of the estimation errors as discussed later.

a) Assumptions for DG estimation:

- 1) Power flow measurements at the resolution of 1 minute is considered. However, the redundancy of the measurements increases if measurements are obtained at faster rate, thereby resulting in better estimation.

- 2) Wind speed observed in whole distribution network is only differed by certain uncertainties. This implies that if the wind speed measured at DSO (or at the location where LSA-DG is hosted) is v_W then wind speed observed at any other location in the network is $v_W + \eta_W$ where η_W is a gaussian distribution of error with $\mu = 0$ and $\sigma = 4\%$
- 3) Solar insolation observed in whole distribution network is only differed by certain uncertainties. This implies that if the solar insolation measured at DSO is I_S then solar insolation observed at any other location in the network is $I_S + \eta_S$ where η_S is a gaussian distribution of error with $\mu = 0$ and $\sigma = 4\%$
- 4) These assumptions do not take in consideration of local phenomena such as clouds, wakes, etc. However, if the amount of DG installed in the distribution network is sufficiently large, the effects of these local phenomenon can be neglected without introducing large error.
- 5) WT connected to each feeder is modelled as aggregated generation as integral of 500 kW generation. This means that if the total WT connected to feeder i is 5 MW then it can be assumed that the feeder has 10, “500 kW equivalent WT” connected to it.
- 6) Similarly, total PV connected to each feeder is modelled as aggregated generation as integral of 100 kW generation. This means that if total PV connected to feeder i is 5 MW then it can be assumed that the feeder has 50, “100 kW equivalent PV panels” connected to it.
- 7) No other types of DGs are considered in the system. Distributed generations such as diesel generators, biomass, fuel cells etc. can be neglected since the volume of these generations are in general considerably smaller compared to wind and PV in most of the distribution networks.
- 8) Consumption is assumed to be constant for the selected time window. The total consumption of the distribution network is equal to the consumption forecast from the TSO which is modelled with gaussian error η_C with $\mu = 0$ and $\sigma = 2\%$
- 9) Large DGs (large wind farms, CHPs etc.) are generally connected to dedicated feeders which are exempted from load shedding. It is assumed that feeder with industrial loads (Fig. 3) represents all those feeders which are not considered for load shedding.

b) *Unknowns*: Number of unknowns for the 10 feeders in each distribution network is:

- $[n_{C,1}, \dots, n_{C,10}]$: Amount of consumptions connected to each feeder
- $[n_{W,1}, \dots, n_{W,10}]$: Number of 500 kW equivalent wind turbines connected to each feeder
- $[n_{S,1}, \dots, n_{S,10}]$: Number of 100 kW equivalent PV panel connected to each feeder
- The unknown vector $\underline{n} = [n_{C,1}, \dots, n_{C,10}, n_{W,1}, \dots, n_{W,10}, n_{S,1}, \dots, n_{S,10}]$ is constituted

However, it should be noted that if there is no installed wind or PV generation to feeder i , then corresponding unknown

$n_{W,i}$ or $n_{S,i}$ should be removed. The maximum number of unknowns in each distribution network is therefore, 30.

c) *Measurement vector*:

- $[P_{m,1,t}, \dots, P_{m,10,t}, P_{m,1,t+1}, \dots, P_{m,10,t+1}, \dots, P_{m,10,t+4}]$: Power flow measurements for all the feeders for 5 minutes.
- $[C_{f,\Sigma}]$: Total consumption forecast of the network
- $[n_{W,\Sigma}]$: Total numbers of 500 kW wind turbine equivalent connected to the network
- $[n_{S,\Sigma}]$: Total numbers of 100 kW PV panel equivalent connected to the network
- The measurement vector $\underline{g} = [P_{m,1,t}, \dots, P_{m,10,t+4}, C_{f,\Sigma}, n_{W,\Sigma}, n_{S,\Sigma}]$ is constituted

Therefore, the number of elements in the measurement vector \underline{g} is 53 ($size_g$) whereas, the number of unknowns are 30 ($size_n$), which makes the system a over-determined system.

d) *Constraints*:

- Lower Bound: \underline{lb} = a zero vector of length n , since all the unknowns can have only positive or zero values
- Upper Bound: \underline{ub} = Installed capacities of each unknown

e) *Equations*:

$$\begin{aligned}
 C_1 - W_{1,t} - S_{1,t} &= P_{m,1,t} \\
 C_2 - W_{2,t} - S_{2,t} &= P_{m,2,t} \\
 \dots &\dots \\
 C_{10} - W_{10,t} - S_{10,t} &= P_{m,10,t} \\
 C_1 - W_{1,t+1} - S_{1,t+1} &= P_{m,1,t+1} \\
 \dots &\dots \\
 C_{10} - W_{10,t+1} - S_{10,t+1} &= P_{m,10,t+1} \\
 C_1 - W_{1,t+2} - S_{1,t+2} &= P_{m,1,t+2} \\
 \dots &\dots \\
 C_{10} - W_{10,t+4} - S_{10,t+4} &= P_{m,10,t+4} \\
 C_1 + \dots + C_{10} &= C_{f,\Sigma} \\
 W_{1,t} + \dots + W_{10,t} &= W_{f,\Sigma} \\
 S_{1,t} + \dots + S_{10,t} &= S_{f,\Sigma}
 \end{aligned} \tag{5}$$

(5) represents the Kirchoff’s Current Law for all the considered feeders for each distribution network. Power flow through each feeder at a given time instant is given as the differences between total consumption and sum of wind and PV generation for that particular feeder. (5) also shows that the total consumption, total wind generation, total PV generation in the distribution network is equal to the consumption forecast, wind forecast and PV forecast for the considered distribution network respectively. It can be observed from (5) that consumptions do not change with time. This is in accordance to assumption 8. By further considering assumptions 5 and 6, (5)

can be written as:

$$\begin{aligned}
 C_1 &= n_{C,1} \\
 \dots & \\
 C_{10} &= n_{C,10} \\
 W_{1,t} &= n_{W,1} * W_{m,t} \\
 \dots & \\
 W_{10,t} &= n_{W,10} * W_{m,t} \\
 W_{1,t+1} &= n_{W,1} * W_{m,t+1} \\
 \dots & \\
 W_{10,t+1} &= n_{W,10} * W_{m,t+1} \\
 \dots & \\
 W_{10,t+4} &= n_{W,10} * W_{m,t+4} \\
 S_{1,t} &= n_{S,1} * S_{m,t} \\
 \dots & \\
 S_{10,t} &= n_{S,10} * S_{m,t} \\
 S_{1,t+1} &= n_{S,1} * S_{m,t+1} \\
 \dots & \\
 S_{10,t+1} &= n_{S,10} * S_{m,t+1} \\
 \dots & \\
 S_{10,t+4} &= n_{S,10} * S_{m,t+4}
 \end{aligned}
 \tag{6}$$

(6) represents the total wind and PV generations for each feeder based on measurements from a 500 kW wind turbine and a 100 kW PV panel placed on a central location. Total generation is equal to total number of equivalent generators multiplied by the measurements. Substituting the values from (6) to (5), including the constraints, and rearranging in matrix form gives;

$$\mathbf{E} * \underline{n} = \underline{g} + \eta \text{ such that } \underline{lb} \leq \underline{n} \leq \underline{ub} \tag{7}$$

where η is the combination of all the errors η_W, η_S, η_C

f) *Solution:* Since (7) is basically a constrained linear least square problem (LLSP) [36], its solution can be found by computing the smallest norm of the error η , i.e.

$$\begin{aligned}
 \min_{\underline{n}} \quad & \frac{1}{2} \|\mathbf{E} * \underline{n} - \underline{g}\|_2^2 \\
 \text{subject to} \quad & \underline{lb} \leq \underline{n} \leq \underline{ub}
 \end{aligned} \tag{8}$$

Feeder Prioritization: The philosophy of providing priorities to feeders is that some of the feeders will have high priority loads like hospitals, traction, dedicated feeder with distributed generation etc. as compared to other feeders. Scores of the feeders can be selected based on following parameters:

- Type of loads connected to the feeder
- Amount of generation connected to the feeder
- Amount of consumption connected to the feeder

Generally, scores or weighage are given by DSOs based on their experiences [34]. In our studies, equal priorities are assumed for all the feeders (except industrial load) based on load type. If there are any priority / weighage among the feeders based on load type, then those weighage can simply be multiplied with assumed scores.

Feeder i is prioritised based on estimated consumption C_i , PV generation S_i and wind generation W_i obtained from the solution of (8). In order to make the prioritization algorithm robust against errors in DG estimation, feeders are only classified into three groups based on their Generation/Consumption

ratio.

Priority or score for each feeder is defined in Table IV, where, generation for feeder i is calculated as $S_i + W_i$ and

TABLE IV
PRIORITIZATION OF FEEDERS BASED ON DG

Generation / Consumption Ratio	Score (S_{C_i})
≤ 0.2	1
0.2 - 0.5	2
≥ 0.5	4

consumption for feeder i is C_i . Scores of all the feeders for the considered distribution system constitutes Score vector, $\underline{S_C}$.

Feeder Selection Algorithm: Feeder selection algorithm discussed with regards to LSA-PF is adjusted here to take Score vector, $\underline{S_C}$ into consideration. Therefore, the cost function in (4) has to be multiplied with Score vector, transforming (4) to (9).

$$\begin{aligned}
 \max \quad & \sum_{i=1}^{total_num_feeders} -S_{C_i,t} * P_{m,i,t} * x_{i,t} \\
 \text{subject to} \quad & \sum_{i=1}^{total_num_feeders} -P_{m,i,t} * x_{i,t} \leq -C_{\Sigma,k,t,shed} \\
 & x_{i,t} \in \{0,1\}
 \end{aligned} \tag{9}$$

This load shedding scheme is expected to provide better frequency response as compared to other load shedding schemes since this scheme prioritizes the feeders with least amount of DG connected for load shedding. Therefore, this method also disconnects minimum amount of DG while disconnecting required amount of consumption.

E. Practical Implementation

While LSA-Directional scheme can be implemented at relay level, LSA-PF and LSA-DG schemes described in this article are developed aiming to have them implemented as centralized control methods at distribution system operator (DSO) control center which can send automated trip signals to the relays connected at the feeders. The measurements and consumption, wind, PV forecasts used in the schemes are either already available or can be made available to transmission system operators through Distributed Generation Management systems [37], Network management solutions [38], etc. These data will have to be transferred to DSOs by TSO. LSA-PF and LSA-DG schemes can obtain measured power flow data from the feeders and use the data from TSO to execute the schemes. Following the computations LSA-PF and LSA-DG schemes can send tripping signals to the relay to the selected feeders. Substation automation infrastructure can be used for data communication. The automation systems generally have fast communication links using IEC 61850 standard [39].

The advantages of LSA-PF and LSA-DG schemes shown in Fig. 4 and Fig. 5 are that feeder selection algorithm, DG estimation, DG prioritization are independent of frequency or RoCoF measurements. As a result, these two schemes can be run independently of disturbances and prioritised list of feeders to be disconnected.

LLSP of (8) is a well known problem of state estimation and has been thoroughly studied and implemented [40], [41]. The advantage of (8) is that number of unknowns are $3 * total_num_feeders$ which is much smaller than number of unknowns in traditional state estimation algorithms.

Time Complexity of “0/1 Knapsack problem” of (4) and (9) can be given by the big O notation as $O(total_num_feeders * C_{\Sigma,k,t,shed})$. Since $C_{\Sigma,k,t,shed}$ is in p.u., it is sufficiently small. Consequently, $O(total_num_feeders * C_{\Sigma,k,t,shed})$ becomes linear and only dependent on number of feeders. For example, if the capacity of distribution network is 2000 MW (and can be chosen as base power); then in order to shed 5% of total consumption in this network, $C_{\Sigma,k,t,shed}$ can have a maximum value of $0.05 * 2000/2000 = 0.05p.u.$. Since, “0/1 Knapsack problem” is an integer programming problem, all the variables are approximated as integers to second decimal point by multiplying them by 100. Therefore, $C_{\Sigma,k,t,shed}$ becomes $0.05 * 100 = 5$. Consequently, time complexity becomes $O(5 * total_num_feeders)$, which is linear. This implies that it is possible to implement LSA-DG for very large distribution systems.

Another important point to note that is the modularity of the schemes. If communication failures happen for the flowchart shown in Fig. 5 and any signal among $W_m, S_m, C_{f,\Sigma}, W_{f,\Sigma}, S_{f,\Sigma}$ is lost, the feeder prioritization can set equal score for all the feeders and the flowchart of Fig. 5 falls back to that of Fig. 4. Similarly, if $C_{f,\Sigma}$ is not available due to some reason, a pre-decided prioritised set of feeders can be selected for tripping and LSA-PF works similar to LSA-Directional. This shows that in case of unavailability of certain signals, the advanced load shedding schemes can always fall back to a simpler load shedding scheme thereby, improving the reliability of the protection system.

IV. RESULTS

In this section, results from the simulations are explained. Performance indices are defined in order to quantify the benefit of using one scheme over another. The different proposed load shedding schemes are compared with respect to frequency responses and these different performance indices.

A. Performance Indices

The following indices are defined in order to evaluate the performance of each scheme:

- **ConsReduction:** This parameter defines the total reduction in consumption in the transmission network which is caused due to load shedding as well as change in frequency. This is defined in p.u. considering 1000 MVA as base MVA.
- **GenReduction:** This parameter defines the total reduction in DG in the transmission network which is caused due to disconnection of feeders during load shedding. This is defined in p.u. considering 1000 MVA as base MVA.
- **FreqNadir:** This is the minimum value of the frequency reached in Hz.

Initially simulation is run for a single time window of 5 minutes. However, in order to validate the performance of the

schemes for all possible wind and PV generation scenarios, Monte Carlo simulation for 400 such time windows are run.

B. Single Time Window

1) *Feeder Selection Algorithm for LSA-PF:* Table V shows generation and consumption for all the feeders for a distribution network for a specific instance for both LSA-PF and LSA-DG.

TABLE V
GENERATION AND CONSUMPTION IN EACH FEEDER FOR LSA-PF AND LSA-DG

i	P_i [MW]	C_i [MW]	$S_i + W_i$ [MW]	LSA-PF Sc_i	LSA-DG Sc_i
1	9.760	10	0.24	1	1
2	8.076	10	1.924	1	1
3	4.147	5	0.853	1	1
4	2.698	5	2.302	1	2
5	2.189	5	2.811	1	4
6	2.952	5	2.048	1	2
7	3.694	5	1.306	1	2
8	3.242	5	1.758	1	2
9	7.917	10	2.083	1	2
10	8.602	10	1.398	1	1

It can be observed from Table V that all the feeders have same priority/score (since generations from DG are not known) based on which “Feeder Selection Algorithm” is run for LSA-PF. The outcome of this algorithm is [0 0 1 0 0 1 0 0 0 0], which means that feeder 3 and feeder 6 should be disconnected.

Therefore, total load disconnected = 10 MW and total generation disconnected = 2.901 MW

2) *DG Estimation for LSA-DG:* Table VI shows the estimated power flow and measured power flow for all the feeders of a distribution network for a specific instance, based on which RMSE and NRMSE are calculated.

TABLE VI
ESTIMATED AND MEASURED POWER FLOW FOR ALL THE FEEDERS FOR A DISTRIBUTION NETWORK

i	$P_{m,i}$	$P_{e,i}$
1	9.76	9.7535
2	8.076	8.2791
3	4.147	4.3070
4	2.698	2.9022
5	2.189	2.3945
6	2.952	3.1573
7	3.694	3.8605
8	3.242	3.4140
9	7.917	7.9675
10	8.602	8.8045

$$RMSE = \sqrt{\frac{\sum_i (P_{m,i} - P_{e,i})^2}{total_num_feeders}} = 0.1713MW$$

$$NRMSE = \frac{RMSE}{(max(P_{m,i}) - min(P_{m,i}))} = 0.0226$$

3) *Feeder Selection Algorithm for LSA-DG:* Table V also shows generation and consumption for all the feeders for a distribution network for a specific instance used for LSA-DG. Priority/score for each feeder (based on Table IV) that can

be observed in Table V is used to run “Feeder Selection Algorithm” for LSA-DG. The outcome of this algorithm is [0 1 0 0 0 0 0 0], which means that feeder 2 should be disconnected.

Therefore, total load disconnected = 10 MW and total generation disconnected = 1.924 MW. Therefore, it can be observed that for the same consumption and generation scenario, LSA-DG disconnects less amount of DG than LSA-PF.

4) *Frequency Response*: In a single time window of 5 min, the frequency response for all the load shedding schemes are compared as shown in Fig. 6 and performance indices are given in Table VII. It can be observed from Fig. 6 that

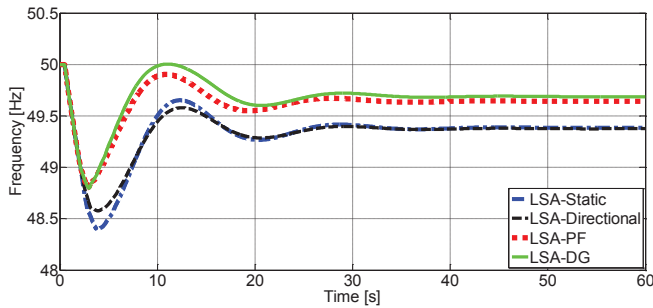


Fig. 6. Frequency responses for different load shedding schemes

FreqNadir values for the LSA-DG and LSA-PF are higher than LSA-Static and LSA-Directional. From the FreqNadir values of Table VII, it can be observed that for LSA-Static, frequency goes down to 48.39 Hz. This implies that there have been 4 stages of load shedding at 49 Hz, 48.8 Hz, 48.6 and 48.4 Hz. The reason for this is quite a lot of generation is disconnected by this scheme as a result the relative load disconnected (given by, ConsReduction-GenReduction) is less. For LSA-Directional consumption shedding is reduced and one less stage of load shedding than LSA-Static can be observed. However, since the frequency nadir is low, it is evident that amount of relative load disconnected in these stages is not adequate. It can be seen from Table VII that although absolute amount of consumptions disconnected are quite high for LSA-Static and LSA-Directional but relative loads disconnected are much less than LSA-PF and LSA-DG. Since, LSA-PF and LSA-DG have similar amount of relative loads disconnected and same number of load shedding stages (at 49 Hz), therefore the frequency responses are quite similar. However, it can be observed that LSA-DG scheme disconnects much less consumption and generation than other schemes.

C. Monte Carlo Simulations

It should be noted that the results shown in Fig. 6 and Table VII are for specific generation and load scenario in a certain time window of 5 minutes. In order to validate the performance over all possible generation scenarios simulations, several wind and solar generation scenarios are randomly generated over a profile of 1 meteorological year. For each of these scenarios, same under-frequency event as discussed

TABLE VII
PERFORMANCE OF DIFFERENT LOAD SHEDDING SCHEMES

Load Shedding Algorithm	ConsReduction		GenReduction		Relative Load Disconnection [p.u.]	FreqNadir	
	Abs. [p.u.]	Improvement over Static Relay [%]	Abs. [p.u.]	Improvement over Static Relay [%]		Abs. [p.u.]	Improvement over Static Relay [Hz]
LSA-Static	1.4288	-	1.0802	-	0.3486	48.39	-
LSA-Direct.	0.862	38.67	0.5055	53.20	0.3565	48.57	0.18
LSA-PF	0.9994	30.05	0.3975	63.20	0.6019	48.81	0.42
LSA-DG	0.7665	46.35	0.1123	89.60	0.6542	48.805	0.415

before is simulated. It should be noted that consumptions are assumed constant for all these simulated scenarios. For each scenario, ConsReduction, GenReduction and FreqNadir values are observed. Maximums, minimums and averages of these performance indices observed over 400 such simulations are shown in Table VIII.

TABLE VIII
PERFORMANCE INDICES FOR 400 SIMULATIONS

Load Shedding Algorithm	ConsReduction			GenReduction			FreqNadir		
	Max. [p.u.]	Min. [p.u.]	Avg. [p.u.]	Max. [p.u.]	Min. [p.u.]	Avg. [p.u.]	Max. [Hz]	Min. [Hz]	Avg. [Hz]
LSA-Static	1.48	0	1.027	1.108	0	0.473	49.06	47.94	48.32
LSA-Direct.	1.22	0	0.724	0.665	0	0.232	49.06	48.32	48.54
LSA-PF	1.025	0	0.712	0.496	0	0.154	49.06	48.35	48.76
LSA-DG	0.907	0	0.461	0.213	0	0.044	49.06	48.62	48.82

It can be observed from Table VIII that LSA-DG performs much better statistically compared to other load shedding schemes.

V. CONCLUSION

The emphasis of this article has been on developing optimal load shedding scheme which disconnects required amount of consumption while disconnecting minimum amount of DG. Different UFLS schemes have been proposed and compared, incorporating static relays, directional relays, power flow and DG data. The results have shown that large penetration of DG can have high impact on system frequency during emergency conditions. The impacts of unintentional disconnection of DG during load shedding on frequency response can be larger frequency dip, more stages of UFLS thereby higher amount of consumption shedding, more DG disconnection, lesser amount of relative load shedding as compared to recommended settings, etc. Novel UFLS scheme considering DG data can prevent extra stages of load shedding, causing minimum generation disconnection and better frequency response as compared to other load shedding schemes. Further studies can be done on comparison of economic impacts of different load shedding schemes. In future, studies can be done to compare

the proposed load shedding schemes with the hybrid load shedding using both frequency and RoCoF settings.

ACKNOWLEDGMENT

The research leading to these results has received funding from the European Union Seventh Framework Programme (FP7/2007-2013) under grant agreement n°. 283012. This work has been done as a part of Innovative Tools for Electrical System Security within Large Areas (iTesla) project. The authors would also like to thank the iTesla TSOs (RTE, ELIA, National Grid, REN, Statnett, IPTO) for providing knowledge about their respective defence plans.

REFERENCES

- [1] Communication from the Commission to the European Parliament and the Council, "Renewable energy: Progressing towards the 2020 target," 2011.
- [2] CIGRE Task Force C2.02.24, "Defense Plans Against Extreme Contingencies," Technical Brochure, April 2007.
- [3] "Technical Background and Recommendations for Defence Plans in the Continental Europe Synchronous Area," Prepared by the Sub Group 'System Protection And Dynamics' Under Regional Group Continental Europe, ENTSO-E, Oct 2010.
- [4] "IEEE Guide for the Application of Protective Relays Used for Abnormal Frequency Load Shedding and Restoration," *IEEE Standard C37.117-2007*, pp. c1-43, 2007.
- [5] B. Delfino, S. Massucco, A. Morini, P. Scalera, and F. Silvestro, "Implementation and comparison of different under frequency load-shedding schemes," in *PES Summer Meeting, 2001*, vol. 1. IEEE, 2001, pp. 307-312.
- [6] P. M. Anderson and M. Mirheydar, "An adaptive method for setting underfrequency load shedding relays," *IEEE Transactions on Power Systems*, vol. 7, no. 2, pp. 647-655, 1992.
- [7] U. Rudez and R. Mihalic, "Analysis of underfrequency load shedding using a frequency gradient," *IEEE Transactions on Power Delivery*, vol. 26, no. 2, pp. 565-575, 2011.
- [8] U. Rudez and R. Mihalic, "A novel approach to underfrequency load shedding," *Electric Power Systems Research*, vol. 81, no. 2, pp. 636-643, 2011.
- [9] V. V. Terzija, "Adaptive underfrequency load shedding based on the magnitude of the disturbance estimation," *IEEE Transactions on Power Systems*, vol. 21, no. 3, pp. 1260-1266, 2006.
- [10] F. Ceja-Gomez, S. S. Qadri, and F. D. Galiana, "Under-frequency load shedding via integer programming," *IEEE Transactions on Power Systems*, vol. 27, no. 3, pp. 1387-1394, 2012.
- [11] W. Luan, M. R. Irving, and J. S. Daniel, "Genetic algorithm for supply restoration and optimal load shedding in power system distribution networks," *IEE Proceedings-Generation, Transmission and Distribution*, vol. 149, no. 2, pp. 145-151, 2002.
- [12] S. Manson, G. Zweigle, and V. Yedidi, "Case study: An adaptive underfrequency load-shedding system," *IEEE Transactions on Industry Applications*, vol. 50, no. 3, pp. 1659-1667, 2014.
- [13] C. Reddy, S. Chakrabarti, and S. Srivastava, "A sensitivity-based method for under-frequency load-shedding," *IEEE Trans. Power Syst.*, vol. 29, no. 2, pp. 984-985, 2014.
- [14] S. Mullen and G. Onsongo, "Decentralized agent-based underfrequency load shedding," *Integrated Computer-Aided Engineering*, vol. 17, no. 4, pp. 321-329, 2010.
- [15] V. Chuvychin and R. Petrichenko, "Development of smart under-frequency load shedding system," *Journal of Electrical Engineering*, vol. 64, no. 2, pp. 123-127, 2013.
- [16] Z. Liu, F. Wen, and G. Ledwich, "An optimal under-frequency load shedding strategy considering distributed generators and load static characteristics," *International Transactions on Electrical Energy Systems*, vol. 24, no. 1, pp. 75-90, 2014.
- [17] D. Xu and A. A. Girgis, "Optimal load shedding strategy in power systems with distributed generation," in *Power Engineering Society Winter Meeting, IEEE*, vol. 2, Columbus, Jan 2001, pp. 788-793.
- [18] A. R. Malekpour, A. R. Seifi, M. R. Hesamzadeh, and N. Hosseinzadeh, "An optimal load shedding approach for distribution networks with dgs considering capacity deficiency modelling of bulked power supply," in *Power Engineering Conference, 2008. AUPEC'08. Australasian Universities*. IEEE, 2008, pp. 1-7.
- [19] P. Mahat, Z. Chen, and B. Bak-Jensen, "Underfrequency load shedding for an islanded distribution system with distributed generators," *IEEE Transactions on Power Delivery*, vol. 25, no. 2, pp. 911-918, 2010.
- [20] C. Z. Mooney, *Monte carlo simulation*. Sage Publications, 1997, vol. 116.
- [21] V. Akhmatov and A. H. Nielsen, "Simulation model of the transmission grid for a large offshore windfarm, used in education and research at the technical university of denmark," *Wind Engineering*, vol. 30, no. 3, pp. 255-263, 2006.
- [22] Ö. Göksu, M. Altin, and P. Sørensen, "Aggregated representation of distribution network models for large-scale transmission network simulations," in *13th International Workshop on Large-Scale Integration of Wind Power into Power Systems*, 2014.
- [23] "Wind turbines. Part 27-1: electrical simulation models for wind power generation wind turbine models, Technical Report IEC 61400-27-1," *International Electrotechnical Commission*, 2015.
- [24] PowerFactory Users Manual, "Digsilent gmbh," *Gomaringen, Germany, May*, 2011.
- [25] K. Das, M. Litong-Palima, P. Maule, and P. E. Sørensen, "Adequacy of Operating Reserves for Power Systems in Future European Wind Power Scenarios," in *IEEE PES General Meeting*, July 2015.
- [26] ELIA, "Solar-PV power generation data." [Online]. Available: <http://www.elia.be/en/grid-data/power-generation/Solar-power-generation-data/Graph>
- [27] ENTSO-E, "Requirements for Grid Connection Applicable to all Generators," 2013. [Online]. Available: https://www.entsoe.eu/fileadmin/user_upload/_library/resources/RfG/130308_Final_Version_NC_RfG.pdf
- [28] Energinet.DK, "Technical regulation 3.2.1 for electricity generation facilities with a rated current of 16 a per phase or lower," Technical report, Tech. Rep., 2011.
- [29] Energinet.DK, "Technical regulation 3.2. 5 for wind power plants with a power output greater than 11 kw," Technical report, Tech. Rep., 2010.
- [30] Energinet.DK, "Technical regulation 3.2.2 for pv power plants with a power output greater than 11 kw," Technical report, Tech. Rep., 2015.
- [31] W. C. New, J. Berdy, P. Brown, and L. Goff, "Load shedding, load restoration and generator protection using solid state and electromechanical underfrequency relays," *General Electric Company, Philadelphia*, vol. 9, 1983.
- [32] NERC, "SERC UFLS Standard: PRC-006-SERC-01." [Online]. Available: <http://www.nerc.com/files/prc-006-serc-01.pdf>
- [33] NERC, "SPP Automatic Underfrequency Load Shedding: PRC-006-SPP-01." [Online]. Available: http://www.nerc.com/docs/standards/rrs/SPP_UFLS_Regional_Standard_Draft%207_clean.pdf
- [34] R. V. Fernandes, S. A. De Almeida, F. P. M. Barbosa, and R. Pestana, "Load shedding Coordination between the Portuguese transmission grid and the Distribution grid with minimization of loss of Distributed Generation," in *PowerTech, 2009 IEEE Bucharest*, 2009, pp. 1-6.
- [35] S. Martello and P. Toth, *Knapsack problems: algorithms and computer implementations*. John Wiley & Sons, Inc., 1990.
- [36] C. L. Lawson and R. J. Hanson, *Solving least squares problems*. SIAM, 1974, vol. 161.
- [37] Energinet.Dk, "Managing the transition towards a sustainable energy system the role of the electricity sector." 2011. [Online]. Available: http://www.cnred.org.cn/english/jsp/download.jsp?fileName=1-Energinet.dl+Presentations_20111020113102.pdf
- [38] Alstom, "Integrating renewable energy resources." [Online]. Available: <http://www.gegridsolutions.com/alstomenergy/grid/Global/Grid/Resources/Documents/Automation/NMS/NMS%20HiRES%20Brochure/Smart%20Grid%20renewable%20Brochure%20GB-epslanguage=en-GB.pdf>
- [39] R. Mackiewicz, "Overview of iec 61850 and benefits," in *Power Systems Conference and Exposition, 2006. PSCE'06. 2006 IEEE PES*. IEEE, 2006, pp. 623-630.
- [40] A. Abur and A. G. Exposito, *Power system state estimation: theory and implementation*. CRC Press, 2004.
- [41] K. Das, J. Hazra, D. P. Seetharam, R. K. Reddi, and A. K. Sinha, "Real-time hybrid state estimation incorporating scada and pmu measurements," in *Innovative Smart Grid Technologies (ISGT Europe), 2012 3rd IEEE PES International Conference and Exhibition on*. IEEE, 2012, pp. 1-8.